Physics 178/278 - David Kleinfeld with Bin Wang -

Winter 2022 Lesson 7

Revised 25 January 2022 10:24

7 Stimulus-Invariant Tuning by Neurons and the 'Ring' Model of Recurrent Interactions. Part 2

We return to our consideration of the "ring" model (Figure 1), as a demonstration of how recurrent connections and the threshold in the gain curve can lead to a powerful computation.

Figure 1: The global model (presented here) and models with local interactions (better suited for the fly) both lead to a moving bump.

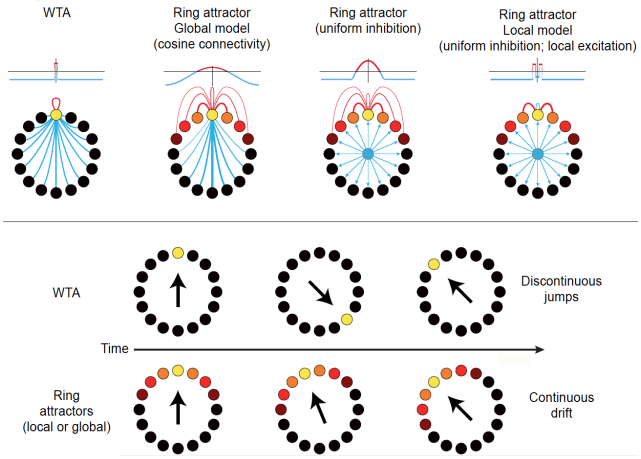

7.0.1 Recap

We previously analyzed this model in the limit of all neurons operating in the linear part of their gain curve, for which

$$\tilde{r}(\phi) = I_0 \left[\frac{1+\epsilon}{1-W_0} + \frac{2\epsilon}{2-W_1} cos(\phi - \phi_0) \right] \tag{7.1}$$

and the selectivity of the output is

$$\begin{aligned} \textbf{Selectivity of output} &\equiv \frac{|r_1|}{r_0} \\ &= \frac{1-W_0}{2-W_1} \times \textbf{Selectivity of input}. \end{aligned}$$

In the linear case, the input determines the output. Thus the choice $\epsilon = 0$ will lead to $r_1 = 0$ and no modulation of the neuronal activity, despite the angular dependence of the interactions.Here we infroduce an angular dependence to the activity, a bump along ϕ, by allowing for nonlinearity in the gain functions and the $W_1 > 2$.

7.0.2 Marginal (spontaneous bump) state

In the linear case, the input determines the output. Thus the choice $\epsilon = 0$ will lead to $r_1 = 0$. Now suppose we increase the interaction term W_1 so that $W_1 > 2$. Clearly we have to allow for a nonlinear gain of the input so that some neurons will be on and some off so that the average modulation is bounded.

For simplicity, we take $f[x]$ as threshold linear, i.e.

$$f[x] = [x]_+. \tag{7.2}$$

Then we expect that $|r_1| > 0$ even if $\epsilon = 0$. In this case we expect a bump of neuronal activity that is centered around the average direction of phase, ψ.

$$\begin{aligned} r_1 &= \frac{1}{2\pi}\int_{\psi-\pi}^{\psi+\pi} d\phi' \left[r(\phi')\right]_+ e^{-i\phi'} \qquad (7.3)\\ &= \frac{1}{2\pi}\int_{\psi-\pi}^{\psi+\pi} d\phi' \left[W_0 r_0 + I_0 - \theta + W_1|r_1|cos(\phi'-\psi)\right]_+ e^{-i\phi'}. \end{aligned}$$

The bump is taken to have an extent with a half width of ϕ_C, which we will have to relate to the synaptic weights. Then we can write a self consistency equation

$$\begin{aligned} r_1 &= \frac{1}{2\pi}\int_{\psi-\phi_C}^{\psi+\phi_C} d\phi'([W_0 r_0 + I_0 - \theta + W_1|r_1|cos(\phi'-\psi)] \qquad (7.4)\\ &\quad - [W_0 r_0 + I_0 - \theta + W_1|r_1|\ cos\left(\psi \pm \phi_C - \psi\right)])e^{-i\phi'}\\ &= W_1\ |r_1|\ \frac{1}{2\pi}\int_{\psi-\phi_C}^{\psi+\phi_C} d\phi'\left(cos(\phi'-\psi) - cos\ \phi_C\right)e^{-i\phi'}\\ &= W_1\ |r_1| e^{-i\psi}\frac{1}{2\pi}\int_{-\phi_C}^{\phi_C} dx\left(cos\ x\ -\ cos\ \phi_C\right)e^{-ix}\\ . &= W_1\ r_1\ \frac{1}{2\pi}\int_{-\phi_C}^{\phi_C} dx\left(\frac{e^{ix}}{2}\ +\ \frac{e^{-ix}}{2}\ -\ cos\ \phi_C\right)e^{-ix}\\ &= W_1\ r_1\ \frac{1}{2\pi}\int_{-\phi_C}^{\phi_C} dx\left(\frac{1}{2}\ +\ \frac{e^{-i2x}}{2}\ -\ cos\ \phi_C\ e^{-ix}\right)\\ &= W_1\ r_1\ \frac{1}{2\pi}\left(\phi_C - \frac{1}{2}sin\ 2\phi_C\right) \end{aligned}$$

so that

$$W_1 = \frac{4\pi}{2\phi_C - sin\ 2\phi_C}. \tag{7.5}$$

Our result relates the synaptic strength to the pattern of activation. It means that the network will form a bump of activity with width $\pm\phi_C$. The minimum value of the connectivity, for the widest possible bump with $\phi_C = \pi$, is $W_1 = 2$ (Figure 2). This is just where the network is linear. Further, $\phi_C \to 0$ as $W_1 \to \infty$, i.e., stronger connections yield a narrower bump. In the absence of an input, the phase of the bump is arbitrary.

Figure 2: Tuning width versus W_1

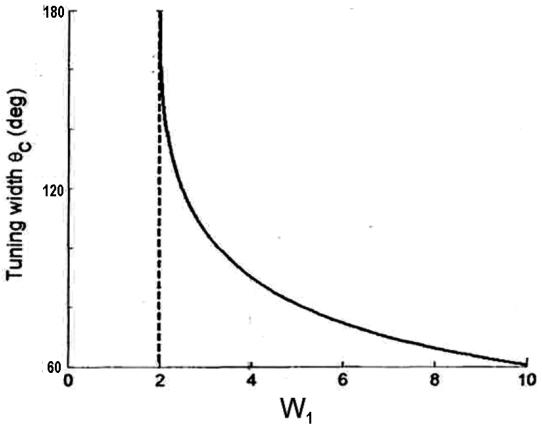

7.0.3 Symmetry breaking by a weak input

A weak input will pin the angular position, or phase, of the bump. Weak means that $0 < \epsilon \ll 1/2$. So long as the stimulus is weak, the tuning does not depend on the stimulus parameters, i.e., on the selectivity of the input. To calculate the selectivity of the output we first need to calculate r_0 similarly to the analysis for the above analysis if r_1. We have

$$
\begin{aligned}
r_0 &= \frac{1}{2\pi}\int_{\psi-\pi}^{\psi+\pi} d\phi' \,[r(\phi')]_+ && (7.6)\\
&= \frac{1}{2\pi}\int_{\psi-\pi}^{\psi+\pi} d\phi' \,[W_0 r_0 + I_0 - \theta + W_1|r_1|cos(\phi'-\psi)]_+ && (7.7)\\
&= \frac{1}{2\pi}\int_{\psi-\phi_C}^{\psi+\phi_C} d\phi' ([W_0 r_0 + I_0 - \theta + W_1|r_1|cos(\phi'-\psi)]\\
&\qquad - [W_0 r_0 + I_0 - \theta + W_1|r_1|\ cos\,(\psi \pm \phi_C - \psi)])\\
&= W_1\ |r_1|\ \frac{1}{2\pi}\int_{\psi-\phi_C}^{\psi+\phi_C} d\phi'\,(cos(\phi'-\psi) - cos\ \phi_C)\\
&= W_1\ |r_1| e^{-i\psi}\frac{1}{2\pi}\int_{-\phi_C}^{\phi_C} dx\,(cos\ x\ -\ cos\ \phi_C)\\
. &= W_1\ r_1\ \frac{1}{\pi}\,(sin\phi_C - \phi_C\ cos\phi_C)
\end{aligned}
$$

$$= \quad r_1 \; 4 \; \frac{sin\phi_C - \phi_C \; cos\phi_C}{2\phi_C - sin \; 2\phi_C}.$$

so that unlike the case for linear response, the average activity tracks the modulated activity. Thus we have

$$\begin{aligned} \textbf{Selectivity of output} \quad &\equiv \quad \frac{|r_1|}{r_0} \\ &= \quad \frac{1}{4} \; \frac{2\phi_C - sin2\phi_C}{sin\phi_C - \phi_C \; cos\phi_C}, \end{aligned} \tag{7.8}$$

which varies between 1/2 and 1, i.e., by very little, as a function of ϕ_C. In this sense, the network will amplify a weak input and drive a response. Unlike the case of a feedforward network, where the width of the tuning curve depends on the input parameters I_0 and ϵ, here the width depends only on W_1. This satisfies the goal of invariance. The relation of W_1 to the width of the tuning curve constitutes a design rule for invariant tuning (Figure 3). There are also a restricted set of values of W_0 and W_1 that satisfy stability of the output (Figure 4).

Figure 3: Selectivity of the network as a function of W_1

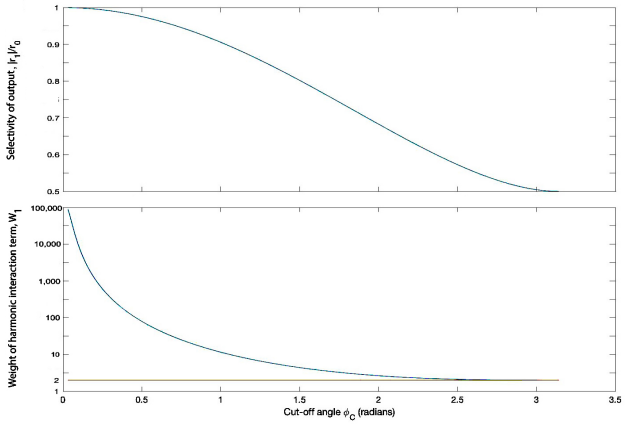

7.1 Epilog

The ring model was motivated by experiments on the coding of orientation in visual stimuli. A number of predictions were made.

Contrast invariance: This is observed and was a motivation observation (Figure 6).

Transient onset of invariance: The invariance should arise slowly as this depends on recurrent connections. Thus the response of neurons at short times is expected to follow feedforward

Figure 4: Phase diagram for different ranges of synaptic weights

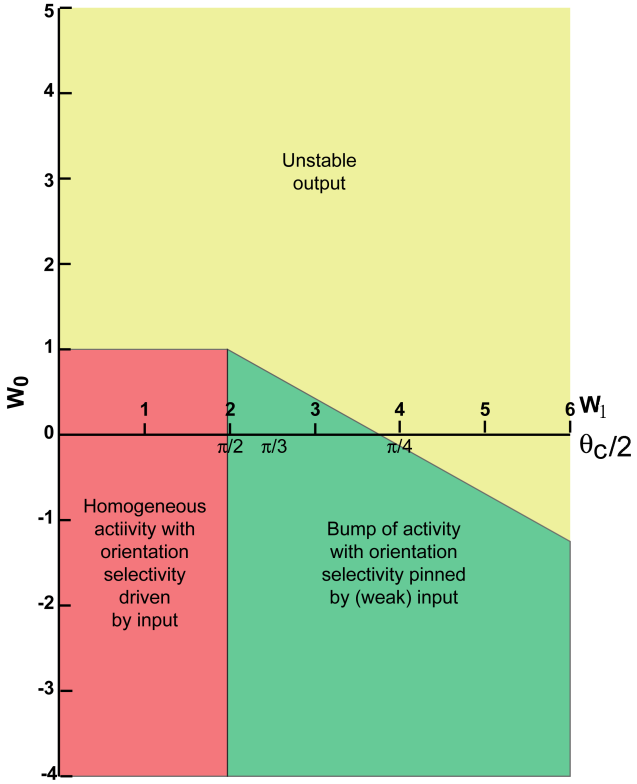

dynamics, while the response at later times, say after tens of milliseconds, would follow recurrent dynamics. This was not found.

Moving bump: Recordings from the colliculus for eye position and from the anterior thalamus for heading suggest the notion of a moving bump of activity. This was predicted to occur in the visual system when the angle of the stimulus is rapidly changes. Here, activity would transiently pass through neurons that coding intermediate orientations (Figure 5). This was not found to date in V1 cortex, yet is seem nicely in the fly ellipsoid body (Figure 7).

Angular dependent connectivity: This is really a postdiction. Neurons with similar orientation preference tend to make stronger connections. Ditto for neurons in the same direction.

The great success of the model turns out to be with respect to heading, as seen in the activity of neurons in the ellipsoid body of the central complex of the fly and their manipulation by optogenetics (Figure 8). Neurons will code their preferred heading relative to

Figure 5: Evolution of neuronal activity in response to a shift in stimulus orientation from 0 to 60 degrees. From Hansel and Sompolinsky 1998.

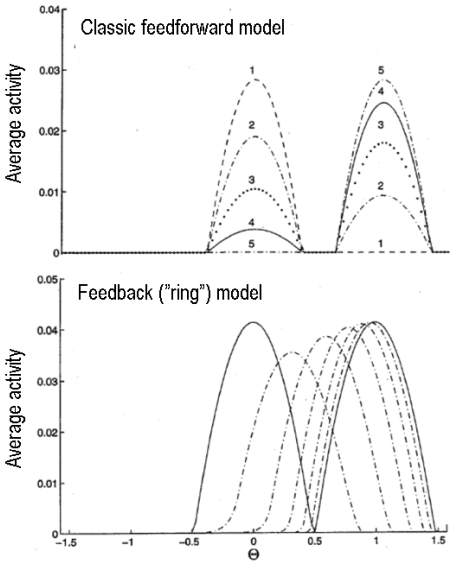

Figure 6: Contrast invariance with feedback. W_0 = -0.4, W_1 = 4.0, and ϵ = 0.09. From Hansel and Sompolinsky 1998.

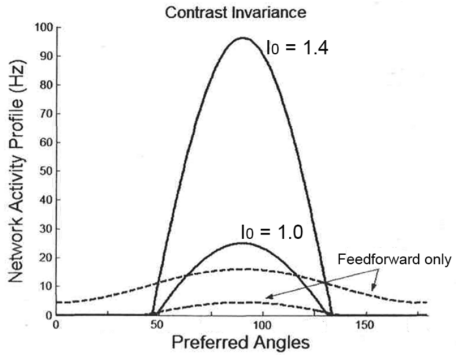

the direction - call it ϕ_0 - of a landmark. Modifications of the ring model that more closely match the observed anatomy have been analyzed (Figure 1). Other work is trying to see if these models hold, in some fashion, for three-dimensional movement (Figure 9).

7.1.1 Travel versus heading: A final calculation by the fly

We are done with the essence of the ring model, but from an ethological perspective the fly needs to compute its direction travel as opposed to just the heading. The travel direction, denoted Ω, includes shifts in direction of heading caused by wind. Recent work provides a basis for this calculation, which we will sketch. The problem is illustrated in Figure 10; there are for four populations of neurons that code for wind direction, the PreFan body neurons (PF-Ns) neurons, that target neurons in the Fan-shaped body.

Figure 7: Evolution of neuronal activity in response to a shift in landmark. From Kim, Rouault, Druckmann and Jayaraman 2017.

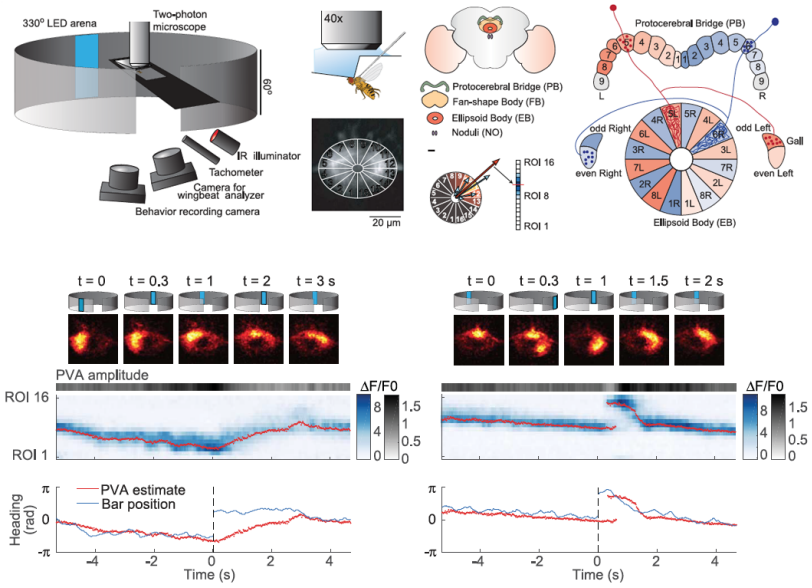

Figure 8: Optiogenetic activation of heading cells leads to a stable state. From Kim, Rouault, Druckmann and Jayaraman 2017.

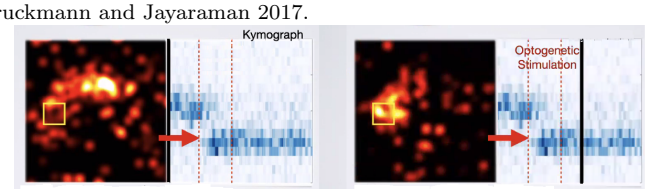

These are tuned to wind direction, but not heading (Figure 11). Heading and wind direction and heading come together in the Fan-shaped body, and the question is how travel is computed (Figure **??**). These neurons have responses whose amplitude depend on wind velocity, i.e., speed $|bfV|$ and direction Θ, and that code the direction of travel direction, denoted Ω as well.The four flavors of input can be described as

$$\text{Rate of PF} - \text{N}_{\text{dL}} \text{ input} = |V| \sin\Omega \cos(\Theta - \phi + \pi/4) \quad (7.9)$$

$$\text{Rate of PF} - \text{N}_{\text{dR}} \text{ input} = |V| \cos\Omega \cos(\Theta - \phi - \pi/4) \quad (7.10)$$

$$\text{Rate of PF} - \text{N}_{\text{vL}} \text{ input} = -|V| \sin\Omega \cos(\Theta - \phi - 3\pi/4) \quad (7.11)$$

$$\text{Rate of PF} - \text{N}_{\text{vR}} \text{ input} = -|V| \cos\Omega \cos(\Theta - \phi + 3\pi/4) \quad (7.12)$$

Nature supplies a number of phase shifts through anatomical positioning of different copies of the inputs to $h\Delta B$ neurons. in the Fan Shaped Body (Figure 12); this turns out to be critical for summation of trigonometric functions! The output from these four cells are added together in the Fan Shaped Body and used to

Figure 9: The ring model can be extended to describe coding in two and even three dimensions, as occurs in the heading of flying animals, such as bats

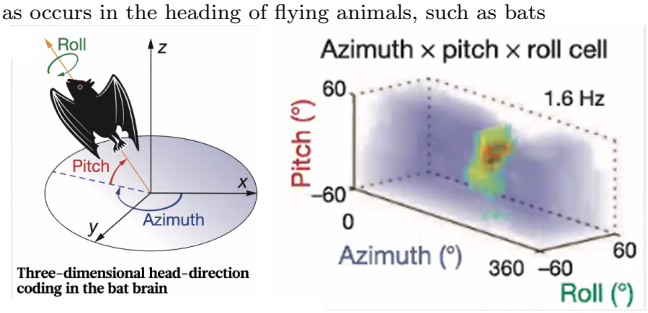

Figure 10: The travel direction complex of fly. From Lyu, Abbott and Maimon, Nature 2021

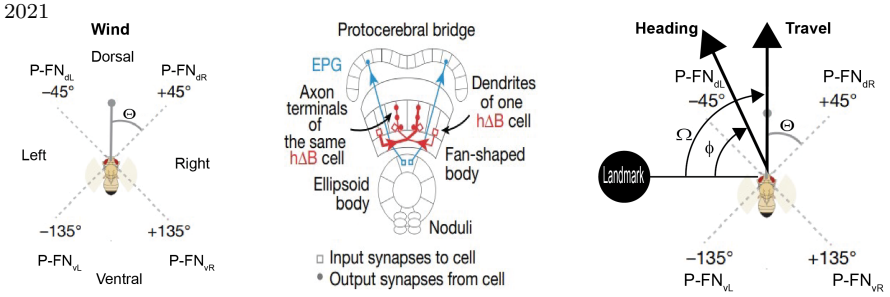

compute the direction of heading. All we need to recall to simply this summation is that $\cos(A+B) = \cos A \cos B$ - $\sin A \sin B$ and that $cos(\pi/4) = sin(\pi/4) = 1/\sqrt{2}$. Then

$$\text{Sum of rates of PF} - \text{N inputs} = \frac{|V|}{\sqrt{2}} \left[\sin\left(\Omega + \Theta - \phi\right) + \cos\left(\Omega + \Theta - \phi\right)\right]. \tag{7.13}$$

This is maximum when the derivation is zero, or $\cos\left(\Omega + \Theta - \phi\right)$ $= \sin\left(\Omega + \Theta - \phi\right)$, or $\Omega + \Theta - \phi = \pi/4$. Thus if different neurons code different values of Ω, the rate is greatest for the cell with

$$\Omega = \phi - \Theta + \frac{\pi}{4}. \tag{7.14}$$

So the fly knows its travel direction, using information based on heading and wind direction, by the index of the neuron with the largest rate (Figure 10).

Figure 11: The response of PR-N neurons to changes in wind direction (top and middle row) and the lack of response with respect to changes in heading (bottom row). Note $\pm\pi/4$ and $\pm 3\pi/4$ shifts in physiological output (Figure 12). From Lyu, Abbott and Maimon, Nature 2021

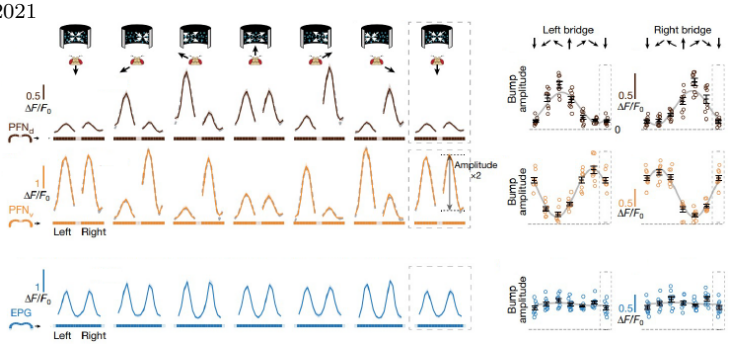

Figure 12: The direction complex of fly showing $\pm\pi/4$ and $\pm 3\pi/4$ anatomical offsets. From Lyu, Abbott and Maimon, Nature 2021